Letter

Discovery of Highly Potent 2-Sulfonyl-Pyrimidinyl Derivatives for Apoptosis Inhibition and Ischemia Treatment

Li Li, Xian Jiang, Shaoqiang Huang, Zhengxin Ying, Zhao-Lan Zhang, Chenjie Pan, Sisi Li, Xiaodong Wang, and Zhiyuan Zhang

ACS Med. Chem. Lett., **Just Accepted Manuscript** • DOI: 10.1021/acsmedchemlett.6b00489 • Publication Date (Web): 01 Mar 2017

Discovery of Highly Potent 2-Sulfonyl-Pyrimidinyl Derivatives for Apoptosis Inhibition and Ischemia Treatment

Li Li[§,†], Xian Jiang[†], Shaoqiang Huang[†], Zhengxin Ying[†], Zhaolan Zhang[†], Chenjie Pan[†], Sisi Li[†], Xiaodong Wang[*,†] and Zhiyuan Zhang[*,†,#]

[§]School of Life Sciences, Peking University, Beijing, 100871, China

[†]National Institute of Biological Sciences (NIBS), Beijing, 102206, China

[#]Collaborative Innovation Center for Cancer Medicine,Beijing, 102206, China

KEYWORDS. Apoptosis inhibitors; phenotypic screen; structure-activity optimization; ischemia treatment; mitochondria protection.

ABSTRACT: A series of 2-sulfonyl-pyrimidinyl derivatives was developed as apoptosis inhibitors. These represent the first class of apoptosis inhibitors that function through stabilizing mitochondrial respiratory complex II. Starting from a phenotypic screen hit with micromolar activity, we optimized the cellular apoptosis inhibition activity of 2-sulfonyl-pyrimidinyl derivatives to picomolar levels. The therapeutic potential of these new apoptosis inhibitors was further demonstrated by their neuroprotective effect on an ischemic animal model.

Excessive apoptosis is closely associated with immunodeficiency diseases, liver diseases, ischemia-associated injury, and neurodegenerative diseases, including Alzheimer's syndrome, Parkinson's syndrome, Huntington's syndrome, and amyotrophic lateral sclerosis.[1-7] Upon recognition of stimulus signals that initiate mitochondria-mediated apoptosis, the decision of whether or not to initiate apoptosis is determined via the complicated regulation of pro- and anti-apoptotic BCL-2 (B-cell lymphoma-2) protein family members.[1] BH-3 only proteins (tBid, Bim, etc) trigger the conformational activation of Bax and/or Bak, which in turn oligomerize and translocate to the mitochondrial outer membrane and lead to mitochondrial permeability changes.[1,8] These changes enable the release of pro-apoptotic proteins such as cytochrome c and Smac to the cytoplasm.[1,8,9] These pro-apoptotic factors then mediate the activation of caspases and ultimately lead to cell death.

The great majority of research into apoptosis inhibitors has focused on targeting caspases or proteins of the pro-apoptotic BCL-2 family.[10] Blocking caspase activity can stop the final execution step of apoptosis, but, by this stage, cells have already suffered considerable damage that typically induces other types of cell death such as necrosis.[11,12] Bax and Bid inhibitors have been developed to target apoptosis.[13-16] However, these apoptosis inhibitors have only moderate potency, with EC_{50} values above or around the micromolar level. Additionally, blocking a single pro-apoptotic BCL-2 protein may have only limited effects because other pro-apoptotic BCL-2 family proteins are known to have complementary functions.[1,8,9] Therefore, there is an urgent need to develop more efficient apoptosis inhibitors.

In this work, we report the medicinal chemistry effort in the development of a series of 2-sulfonyl-pyrimidinyl derivatives as highly potent apoptosis inhibitors. Starting from a phenotypic screen hit compound with micromolar activity, we optimized the cellular apoptosis inhibition activity in a series of derivative compounds to picomolar level. We also revealed the neuroprotective effect of this class of compounds in a transient focal cerebral ischemia model, further demonstrating their therapeutic potential in treating diseases related to excessive apoptosis. To our knowledge, this class of apoptosis inhibitors is by far the most potent apoptosis inhibitors reported.

Besides, by chemical genetic methods using one of these compounds (compound **33**, also named compound A), we recently reported the identification of the succinate dehydrogenase subunit B (SDHB) of mitochondrial respiratory complex II as the target protein, which is also a new target for apoptosis inhibition.[17] Compound 33 inhibits apoptosis by stabilizing mitochondrial respiratory complex II and protecting the integrity of the mitochondrial electron transport chain.[17] Together, we revealed a class of new and potent apoptosis inhibitors that act on a novel target in the apoptosis signaling pathway, and demonstrated their therapeutic potential in excessive apoptosis-related disease models.

A chemical library containing 200,000 small molecules was screened for compounds that block apoptosis in a cell

line (U2OS_Bim) where overexpression of a pro-apoptotic BCL-2 member Bim is induced by Doxycycline (DOX).[18] Several active hits were identified and further confirmed as having EC_{50} values below 20 μM for maintaining cell survival following Bim-induced apoptosis. All screening hits were resynthesized, and their bioactivities were re-confirmed. Of these hit compounds, N-(2-hydroxy-5-methylphenyl)-4-((4-(thiophen-2-yl)-6-(trifluoromethyl) pyrimidin-2-yl)sulfonyl)butanamide (Fig. 1a, EC_{50}=4.0 μM) could prevent mitochondrial cytochrome c release (Fig. 1b), which could not be achieved by caspase inhibitor zVAD. This indicated the 2-sulfonyl-pyrimidinyl compound functions upstream of caspase activation, and between BCL-2 family member regulation and cytochrome c release. Therefore, this compound was selected for further study.

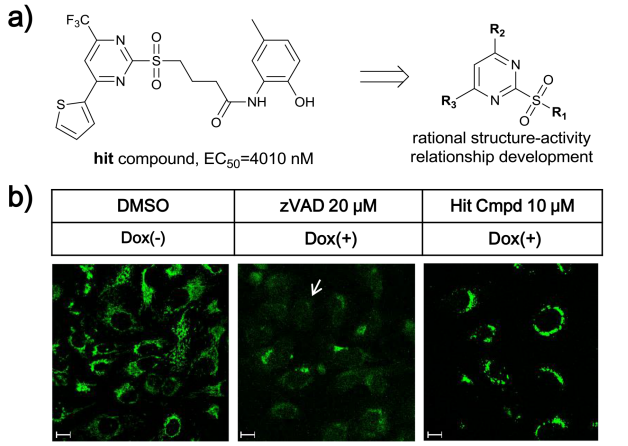

Figure 1. The hit compound identified from a phenotypic screen of apoptosis inhibition can block mitochondrial release of cytochrome c after Dox induced apoptosis. (a) Structure and apoptosis inhibiton activity of the hit compound, and the the side groups (R_1, R_2, and R_3) targeted in SAR development. (b) Immunofluorescence imaging of cytochrome c after treatment with the indicated compounds. The arrow on the middle column indicated an example of cytochrome c release. Scale bar: 20 μm.

To obtain more potent compounds to be used as both target identification tools and potential drug candidates, we undertook rational structure-activity relationship (SAR) optimization. We started by optimization of fragment R_1 (Table 1). In each case, replacement of R_1 with aliphatic groups of varying sizes increased the apoptosis inhibition activity by 3-5 fold (compounds **1**-**3**). Aromatic substitutes were also tested (compounds **4**,**5**), and their activities were similar to that of the hit compound. These results indicate that fragment R_1 was able to tolerate a relatively large change in its structure and maintain the activity. Because compound **1** had the strongest apoptosis inhibition activity, we replaced the original structure of R_1 with a methyl group for further SAR optimization of other parts of the molecule (R_2 and R_3, Figure 1).

We next substituted the $-CF_3$ group at the R_2 position with different groups (compounds **6**-**9**); all such substitutions led to the total loss of activity (Table 1). This may be related to either a constrained binding environment or the necessity for the strong electron withdrawing property of the original $-CF_3$ group.

Table 1. SAR study of compounds **1**-**20**

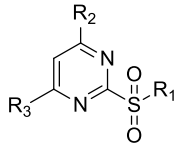

No.	R_1	R_2	R_3	EC_{50} (nM)[a]
1	–Me	$-CF_3$		749 ±11
2	–Et	$-CF_3$		1428 ±291
3	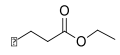	$-CF_3$		1135 ±242
4	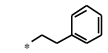	$-CF_3$		1591 ±206
5	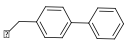	$-CF_3$		4207 ±651
6	–Me	–Me		>20000
7	–Me	$-N_3$		>20000
8	–Me			>20000
9	–Me			>20000
10	–Me	$-CF_3$		2201 ±238
11	–Me	$-CF_3$		6642 ±1261
12	–Me	$-CF_3$		3487 ±418
13	–Me	$-CF_3$	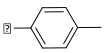	6355 ±469
14	–Me	$-CF_3$	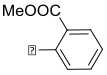	7033 ±421
15	–Me	$-CF_3$	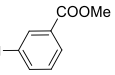	3516 ±446
16	–Me	$-CF_3$	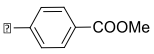	>20000
17	–Me	$-CF_3$	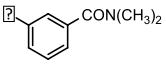	>20000
18	–Me	$-CF_3$	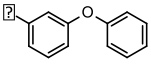	8756 ±1213
19	–Me	$-CF_3$	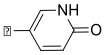	>20000
20	–Me	$-CF_3$	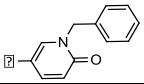	1157 ±66

(a), EC_{50}: cellular apoptosis inhibition on U2OS_Bim cell line.

We next conducted SAR optimization of fragment R_3 (Table 1). Although the replacement of the original thiophene group with phenyl rings (compound **10**) resulted in decreased activity, it offered more options for testing the

influence of substituents on different positions of the ring. Compounds with $-CH_3$ and $-COOCH_3$ substitutions at the 2-, 3-, and 4-positions of the phenyl ring had divergent activities (compounds **11**-**16**). Substitutions at both the 2- and 4-positions (compounds **11**, **13**, **14**, **16**) led to decreased activity compared with compound **10**, whereas substitutions at the 3-position (compounds **12**, **15**) resulted in EC_{50} values similar to **10**. This suggested more open space around the 3-position of the phenyl group. Compound **17** with a $-CON(CH_3)_2$ group had a complete loss of activity, probably because of its polarity or unfavourable conformation. Though compound **18**, which has a 3-oxybenzene group, had a 3-fold decrease in activity compared with compound **10,** the result agreed with our assumption on more open space at this direction and encouraged us to do further SAR morphing at this position. Considering the convenience of modification and synthesis, we chose to replace the original thiophene group at the R_3 position with the pyridone ring (compound **19**) as an intermediate for further SAR exploration of the 3-position. Compound **19** had no activity, possibly because of the polarity of the pyridone ring. However, by adding a benzyl group to the N atom of the pyridone we got compound **20,** of which the activity increased by 2-folds compared with **10**. This result further confirmed that a hydrophobic pocket has been reached by the addition of benzyl group.

Encouraged by the result, SAR exploration on the benzyl ring was then performed in more detail (Table 2). The effects of chloro-substitution at different positions of the benzyl ring (compounds **21**-**23**) were evaluated. The 3- and 4-chloro substitutions of the benzyl ring (compounds **22**, **23**) led to increased apoptosis inhibition activity. We next focused on substitutions at these two positions. Compound **24**, which has a 3-OH substitution, had the same activity as compound **20** and was less potent than the 3-chloro compound **22**, which suggested a hydrophobic environment around the benzyl ring. The 3-OMe substitution of the benzyl ring (compound **25**) increased activity by about 20-fold compared with compound **20**. The –OEt and –OPr substituted compounds **26** and **27** displayed similar activities to that of compound **25**. We subsequently examined the influence of 4-OMe substitution (compound **28**) and found that it increased activity by 12-fold compared with compound **20**, similar to the increase observed for compound **25**. In addition to oxyalkyl substitution, we also tested the activities of ethynyl and cyano groups at the 3- and 4- positions of the benzyl ring (compounds **29**-**32**). Only compound **30**, which has an ethynyl substitution at the 4-position of the benzyl ring, had an increase in activity compared with compound **20**, and this increase was mild. Ethynyl substitution at the 3-position and cyano substitution at both positions led to diminished activity. Based on these results, we next combined the 3- and 4- position –OMe substitutions in compound **33** (compound A), which showed yet a further increase in apoptosis inhibition activity, with an EC_{50} as low as 25 nM. Thus compound **33** is 150-fold more potent than the initial hit compound.

Table 2. SAR study of compounds **21-33**

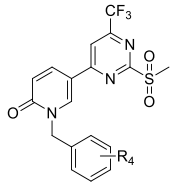

No.	R_4	EC_{50} (nM)[a]
21	2-Cl	**1143±235**
22	3-Cl	**257±37**
23	4-Cl	**66±4.2**
24	3-OH	**1821±371**
25	3-OMe	**57±1.7**
26	3-OEt	**110±25**
27	3-OPr	**69±9.7**
28	4-OMe	**94±9.6**
29	3-ethynyl	**4477±1040**
30	4-ethynyl	**817±189**
31	3-cyano	**4060±477**
32	4-cyano	**3489±184**
33b	3,4-dimethoxy	**25±0.57**

(a), EC50: cellular apoptosis inhibition in the U2OS_Bim cell line.
(b), compound A.

To better understand the structural requirements for activity and to further optimize potency, we undertook a second round of SAR optimization at the original R_1 position (Table 3). Because the previous SAR analysis suggested a large tolerance for various structures, we focused on testing if extension of the R_1 fragment could improve activity.

We first replaced the methyl group in compound **33** with *n*-pentyl and *n*-heptyl groups (compounds **34** and **35**), but lengthening the alkyl chain largely reduced cellular activity. Ether structures (compounds **36** and **37**) were then tried; however, these did not improve the cellular activity much, either. An amide structure was then tested. Compound **38**, which has *N*, *N*-dimethylbutyramide at the R_1 position, had an EC_{50} of 164 nM; this is a mild increase compared with the activities of compounds **36** and **37**. Replacement of the dimethylamine with pyrrolidine (**39**) further increased the activity by ~5-fold compared with compound **38**. We then tried the piperidine at the amide bond (compound **40**), and activity increased dramatically to an EC_{50} of 1.4 nM, which is much higher than observed for compounds **33** and **39**. These observations indicate that large aliphatic moieties at the amide position are favorable for activity, and we speculate that the extended R_1 moiety possibly interacts hydrophobically with the target protein. Consistent with our assumption, the introduction of an unsubstituted amide, a butyramide structure, at R_1 (compound **41**), was detrimental to activity. Therefore, to increase the hydrophobicity of the R_1 fragment, we synthesized compound **42**, which has a highly hydrophobic adamantane moiety. The activity of this compound increased to an EC_{50} of 0.42 nM, which is 50-fold higher than the parent compound **33.**

Table 3. SAR study of compounds **34-42**

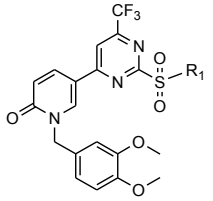

No.	R_1	EC_{50} (nM)[a]
34		364±13.4
35	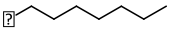	253±17.5
36	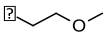	216±20.9
37	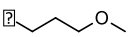	282±27.9
38	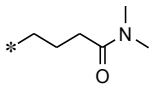	164±12.5
39	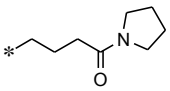	27±2.43
40	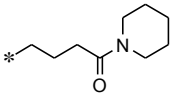	1.4±0.19
41	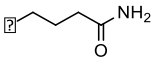	>20000
42	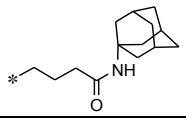	0.42±0.05

(a), cellular apoptosis inhibiton activity.

In addition to testing the inhibition activity of the 2-sulfonyl-pyrimidinyl derivative compounds on Bim overexpression induced apoptosis, we also evaluated if they could block apoptosis induced by the overexpression of tBid, another pro-apoptotic protein of the Bcl-2 family. Most compounds displayed similar apoptosis inhibition activities, and compound **42** had an EC_{50} of 0.23 nM (Table S1).

By chemical genetic methods using a biotinylated derivative of compound **33** as bioaffinitive probe, we previously reported that compound **33** covalently binds the 243 cysteine of SDHB through an SN_2 substitution at the sulfone position. [17] Sulfone can serve as a good leaving group in SN_2 substitution reactions when linked to electron-withdrawing aromatic rings.[19-21] In the SAR study, we observed that the replacement of -CF_3 at the R_2 position with less powerful electron-withdrawing groups totally abolished activity (Table 1, compounds **6-9**). In model reactions with different nucleophilic reagents (cysteine, lysine, and glutathione) (Figure S1, S2), we observed that compounds **1**, **33** and **42** reacted with cysteine and glutathione but not lysine, whereas compound **6,** of which the electron-withdrawing group -CF_3 was replaced by an electron-donating CH_3, didn't react with any of them. This indicated the reactivity of the sulfone group in the tested compounds was consistent with the cellular activity of the corresponding compounds. We also confirmed that active 2-sulfonyl-pyrimidinyl derivative compounds shared the covalent binding property using a cellular wash/no-wash assay (Table S2).[22] Before apoptosis induction and cell viability determination, two substets of cells were incubated with tested compounds, and then one subset of cells was washed several times to eliminate the unbound test compounds while the other subset of cells was not washed. Tested compounds all had similar EC_{50} values under these two conditions, indicating irreversible binding modes for these compounds.

In addition to blocking mitochondrial-mediated apoptosis, this class of 2-sulfonyl-pyrimidinyl derivative apoptosis inhibitors could also block the dysfunction of mitochondria that occurs following the induction of apoptosis. To evaluate mitochondrial function, we measured changes in mitochondrial membrane potential under different conditions using tetramethylrhodamine methyl ester (TMRM), a membrane potential sensitive red fluorescent dye. Dox induction of Bim overexpression is known to result in the loss of mitochondrial membrane potential and thus diminish TMRM enrichment during apoptosis.[23] All of the tested compounds maintained TMRM enrichment and mitochondria membrane potential, an outcome that cannot be achieved with the caspase inhibitor zVAD (Figure 2a). The mitochondrial protective effect of the 2-sulfonyl-pyrimidinyl derivative apoptosis inhibitors was further supported by measurements of reactive oxygen species (ROS) levels taken following the induction of apoptosis. ROS levels are known to increase the following interruption of the electron transport chain and the resulting changes in membrane permeability that occur during apoptosis. Such ROS increases are understood to be stimulative factors for apoptosis induction and to cause further damage to cells.[24] Treatment with the novel apoptosis inhibitor compounds maintained normal ROS levels, even upon apoptosis induction, in a dose-dependent manner (Figure 2b).

It is now firmly established that excessive apoptotic cell death is prominent in neurological disorders, such as Alzheimer's disease and Parkinson's disease, and it is also a main cause for cerebral ischemic stroke.[25] Following cerebral ischemia, BH3-only proteins are upregulated and activate the intrinsic apoptosis pathway.[26] Compound **33** has already been shown to promote cell survival in a Parkinson's disease model.[17] Here, we tested the potential efficiency of this series of apoptosis inhibitor compounds in a rat transient focal ischemia model.[27] A nylon suture was introduced to occlude the origin of the middle cerebral artery (MCA). A 5μL solution of different concentrations of compound **33** or **42** was injected into the left striatum after suture insertion. The suture was removed 1hr after insertion to allow reperfusion. After 24hr, animals were sacrificed. Evaluation of the brain infarct volume in different groups showed that both compounds **33** and **42** had obvious protective effects on brain tissues and reduced the brain infarct volume due to induction of focal cerebral ischemia (Fig. 3). Consistent with the SAR study, at injection concentrations of 50μM and 200μM, compound **42** had a better protective effect than compound **33.**

In conclusion, using medicinal chemistry we systematically developed a novel and highly potent series of apoptosis

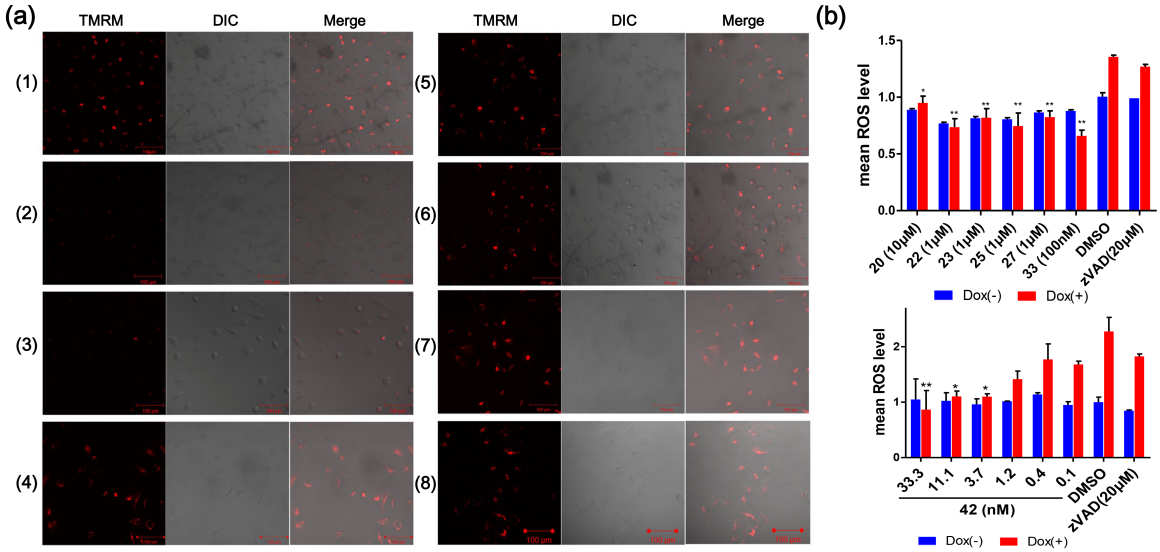

Figure 2. Mitochondrial protective effects of a series of apoptosis inhibitors. (a) TMRM staining of mitochondria in US2OS-Bim cells with (1),no apoptosis induction and treatment with DMSO, and with apoptosis inducted by the addition of DOX in the presence of the following treatments: (2), DMSO; (3), zVAD (10μM); (4), compound **20** (10μM); (5), compound **22** (1μM); (6), compound **23** (1μM); (7), compound **33** (100nM); (8), compound **42** (3 nM). Scale: 100 μm. (b) Mean cellular ROS levels in U2OS-Bim cells with (red bars) and without (blue bars) Dox induced apoptosis under the indicated compound treatments. Top: ROS levels under treatment with various apoptosis inhibitor compounds, DMSO, and zVAD. Bottom: ROS levels under treatment with different concentrations of compound **42**, DMSO, and zVAD (20μM). The error bars represent the standard error of results from two separate experiments. P values are based on comparisons of each sample to the DMSO-treated apoptosis induction group. *: P<0.05; **: P<0.01; ***: P<0.001.

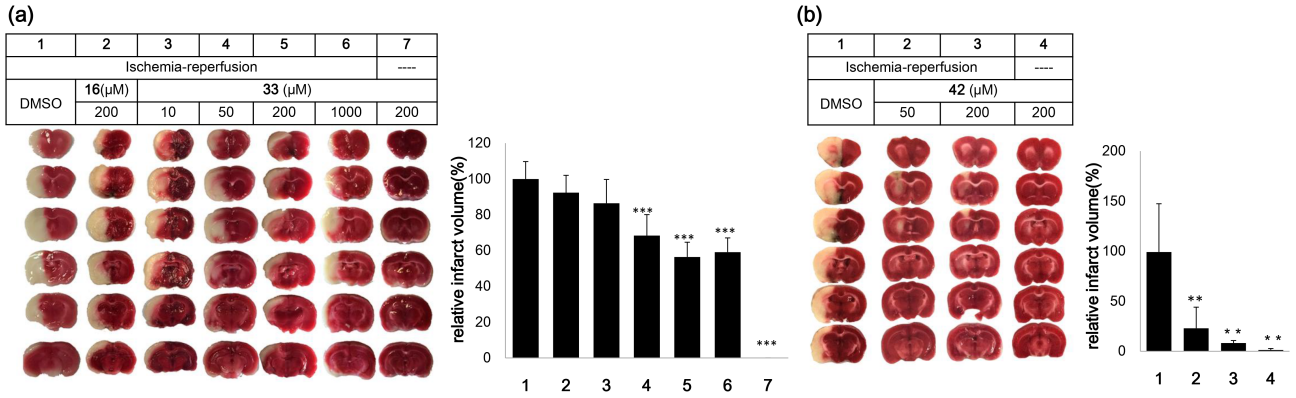

Figure 3. Compound **33**(a) and compound **42** (b) have protective effects against ischemia-reperfusion injury. left: Representative 2, 3, 5-triphenyltetrazolium chloride (TTC) stained sections from middle cerebral artery occlusion (MCAO) brains injected with 5μl of the indicated concentrations of compounds **33** and **42**. The white color represents the infarct and the red color represents the normal tissue. Right: Quantification of relative infarct volume. The numbers 1-7 on the x-axis correspond to the treatments in the top panel. Bars represent means ± standard deviation, n=3-6. P values are based on comparisons of each sample to the DMSO-treated ischemia-reperfusion(+) group.*: P,0.05; **: P<0.01; ***: P<0.001.

inhibitors. Based on an initial hit compound from phenotypic screening, we improved the cellular apoptosis inhibition activity of 2-sulfonyl-pyrimidinyl derivatives from low micromolar to picomolar levels through SAR optimization, and verified their covalent binding mode. This series of compounds showed mitochondrial protective effect as well as apoptosis inhibition. Following our previous work on the identification of SDHB subunit of mitochondrial respiratory complex II as the interacting target of compound **33** and the demonstration of protective effect on Parkinson model, we further showed that compounds **33** and **42** are also highly efficacious on transient focal cerebral ischemia model, indicating the great therapeutic potential in the development of novel therapies to treat apoptosis-related diseases.

ASSOCIATED CONTENT

Supporting Information

Detailed experimental procedure, supporting figures and tables, synthesis and characterization of all compounds and intermediates, are listed in **Supporting Information.** This material is available free of charge via the Internet at http://pubs.acs.org.

AUTHOR INFORMATION

Corresponding Author

*Email: zhangzhiyuan@nibs.ac.cn

Author Contributions

All authors have given approval to the final version of the manuscript.

Funding Sources

This work is supported by National High Technology Project 973 (2011CB504300).

Notes

The authors declare no competing financial interest.

ACKNOWLEDGMENT

We thank Prof. Zhenhua Zhang (China Agricultural University) for providing several azide reagents (synthesized in the National Key Technologies R&D Program of China, 2015BAK45B01, CAU) and Mr. Qinsi Ji for his synthesis work.

REFERENCES

(1) Elmore, S., Apoptosis: a review of programmed cell death. *Toxicologic pathology* **2007,** *35* (4), 495-516.

(2) Wyllie, A. H., "Where, O death, is thy sting?" A brief review of apoptosis biology. *Molecular neurobiology* **2010,** *42* (1), 4-9.

(3) Mattson, M. P., Apoptosis in neurodegenerative disorders. *Nature reviews Molecular cell biology* **2000,** *1* (2), 120-130.

(4) Roshal, M.; Zhu, Y.; Planelles, V., Apoptosis in AIDS. *Apoptosis* **2001,** *6* (1-2), 103-116.

(5) Patel, T.; Roberts, L. R.; Jones, B. A.; Gores, G. J. In *Dysregulation of apoptosis as a mechanism of liver disease: an overview*, Seminars in liver disease, © 1998 by Thieme Medical Publishers, Inc.: 1998; pp 105-114.

(6) Favaloro, B.; Allocati, N.; Graziano, V.; Di Ilio, C.; De Laurenzi, V., Role of apoptosis in disease. *Aging (Albany NY)* **2012,** *4* (5), 330-349.

(7) Choi, D. W., Ischemia-induced neuronal apoptosis. *Current opinion in neurobiology* **1996,** *6* (5), 667-672.

(8) Mayer, B.; Oberbauer, R., Mitochondrial regulation of apoptosis. *Physiology* **2003,** *18* (3), 89-94.

(9) Gross, A., BCL - 2 Proteins: Regulators of the Mitochondrial Apoptotic Program. *IUBMB life* **2001,** *52* (3 - 5), 231-236.

(10) Reed, J. C.; Huang, Z., Apoptosis pathways and drug targets. *Nature Rev Drug Discov* **2004,** *3* (111), 895-981.

(11) Samali, A.; Nordgren, H.; Zhivotovsky, B.; Peterson, E.; Orrenius, S., A comparative study of apoptosis and necrosis in HepG2 cells: oxidant-induced caspase inactivation leads to necrosis. *Biochemical and biophysical research communications* **1999,** *255* (1), 6-11.

(12) Vandenabeele, P.; Vanden Berghe, T.; Festjens, N., Caspase inhibitors promote alternative cell death pathways. *Sci STKE* **2006,** *2006* (358), pe44.

(13) Bombrun, A.; Gerber, P.; Casi, G.; Terradillos, O.; Antonsson, B.; Halazy, S., 3, 6-dibromocarbazole piperazine derivatives of 2-propanol as first inhibitors of cytochrome c release via Bax channel modulation. *Journal of medicinal chemistry* **2003,** *46* (21), 4365-4368.

(14) Hetz, C.; Vitte, P.-A.; Bombrun, A.; Rostovtseva, T. K.; Montessuit, S.; Hiver, A.; Schwarz, M. K.; Church, D. J.; Korsmeyer, S. J.; Martinou, J.-C., Bax channel inhibitors prevent mitochondrion-mediated apoptosis and protect neurons in a model of global brain ischemia. *Journal of Biological Chemistry* **2005,** *280* (52), 42960-42970.

(15) Becattini, B.; Sareth, S.; Zhai, D.; Crowell, K. J.; Leone, M.; Reed, J. C.; Pellecchia, M., Targeting apoptosis via chemical design: inhibition of bid-induced cell death by small organic molecules. *Chemistry & biology* **2004,** *11* (8), 1107-1117.

(16) Becattini, B.; Culmsee, C.; Leone, M.; Zhai, D.; Zhang, X.; Crowell, K. J.; Rega, M. F.; Landshamer, S.; Reed, J. C.; Plesnila, N., Structure–activity relationships by interligand NOE-based design and synthesis of antiapoptotic compounds targeting Bid. *Proceedings of the National Academy of Sciences* **2006,** *103* (33), 12602-12606.

(17) Jiang, X.; Li, L.; Ying, Z.; Pan, C.; Huang, S.; Li, L.; Dai, M.; Yan, B.; Li, M.; Jiang, H., A Small Molecule That Protects the Integrity of the Electron Transfer Chain Blocks the Mitochondrial Apoptotic Pathway. *Molecular Cell* **2016,** *63* (2), 229-239.

(18) Jiang, X.; Jiang, H.; Shen, Z.; Wang, X., Activation of mitochondrial protease OMA1 by Bax and Bak promotes cytochrome c release during apoptosis. *Proceedings of the National Academy of Sciences* **2014,** *111* (41), 14782-14787.

(19) Pfefferkorn, J. A.; Lou, J.; Minich, M. L.; Filipski, K. J.; He, M.; Zhou, R.; Ahmed, S.; Benbow, J.; Perez, A.-G.; Tu, M., Pyridones as glucokinase activators: identification of a unique metabolic liability of the 4-sulfonyl-2-pyridone heterocycle. *Bioorganic & medicinal chemistry letters* **2009,** *19* (12), 3247-3252.

(20) Litchfield, J.; Sharma, R.; Atkinson, K.; Filipski, K. J.; Wright, S. W.; Pfefferkorn, J. A.; Tan, B.; Kosa, R. E.; Stevens, B.; Tu, M., Intrinsic electrophilicity of the 4-methylsulfonyl-2-pyridone scaffold in glucokinase activators: role of glutathione-S-transferases and in vivo quantitation of a glutathione conjugate in rats. *Bioorganic & medicinal chemistry letters* **2010,** *20* (21), 6262-6267.

(21) Kathman, S. G.; Statsyuk, A. V., Covalent tethering of fragments for covalent probe discovery. *MedChemComm* **2016**, *7* (4), 576-585.

(22) Zhou, W.; Hur, W.; McDermott, U.; Dutt, A.; Xian, W.; Ficarro, S. B.; Zhang, J.; Sharma, S. V.; Brugge, J.; Meyerson, M, Settleman, J; Gray, N., A structure-guided approach to creating covalent FGFR inhibitors. *Chemistry & biology* **2010,** *17* (3), 285-295.

(23) Ly, J. D.; Grubb, D.; Lawen, A., The mitochondrial membrane potential (Δψm) in apoptosis; an update. *Apoptosis* **2003,** *8* (2), 115-128.

(24) Circu, M. L.; Aw, T. Y., Reactive oxygen species, cellular redox systems, and apoptosis. *Free Radical Biology and Medicine* **2010,** *48* (6), 749-762.

(25) Dirnagl, U.; Iadecola, C.; Moskowitz, M. A., Pathobiology of ischaemic stroke: an integrated view. *Trends in neurosciences* **1999,** *22* (9), 391-397.

(26) Niizuma, K.; Yoshioka, H.; Chen, H.; Kim, G. S.; Jung, J. E.; Katsu, M.; Okami, N.; Chan, P. H., Mitochondrial and apoptotic neuronal death signaling pathways in cerebral ischemia. *Biochimica et Biophysica Acta (BBA)-Molecular Basis of Disease* **2010,** *1802* (1), 92-99.

(27) Uluç, K.; Miranpuri, A.; Kujoth, G. C.; Aktüre, E.; Başkaya, M. K., Focal cerebral ischemia model by endovascular suture occlusion of the middle cerebral artery in the rat. *JoVE (Journal of Visualized Experiments)* **2011,** (48), e1978-e1978.

Table of Contents

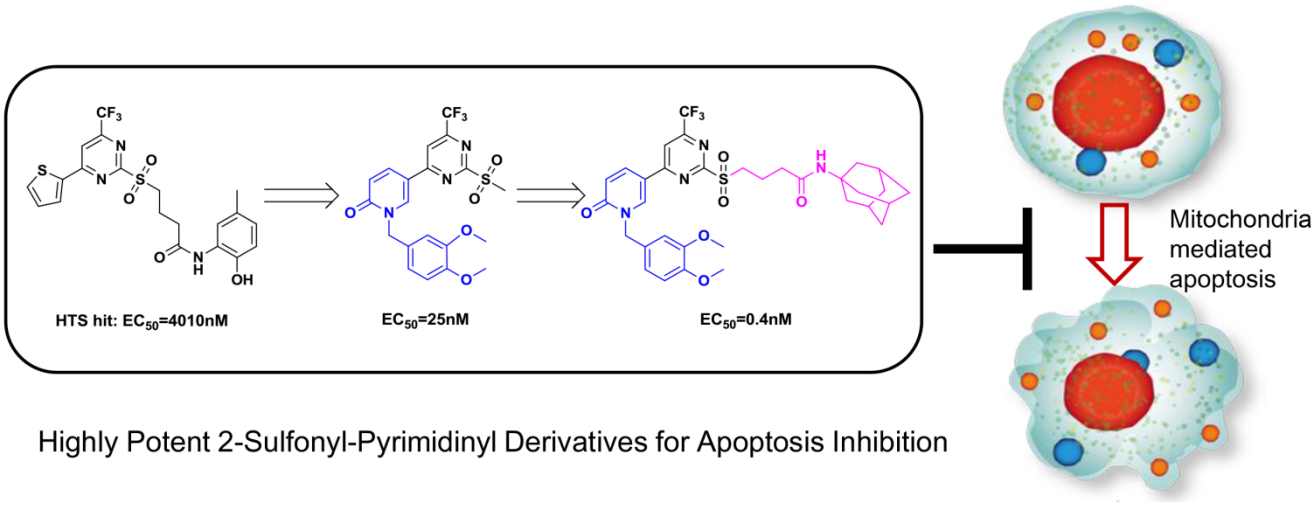

Highly Potent 2-Sulfonyl-Pyrimidinyl Derivatives for Apoptosis Inhibition

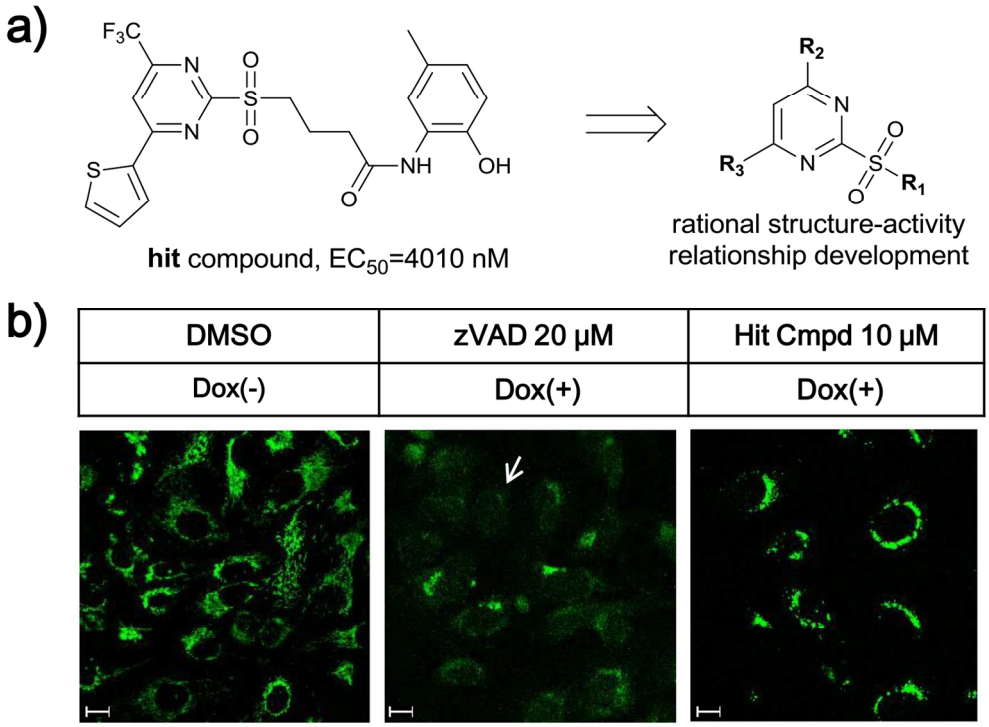

Figure 1. The hit compound identified from a phenotypic screen of apoptosis inhibition can block mitochondrial re-lease of cytochrome c after Dox induced apoptosis. (a) Structure and apoptosis inhibiton activity of the hit compound, and the the side groups (R1, R2, and R3) targeted in SAR development. (b) Immunofluorescence imaging of cytochrome c after treatment with the indicated compounds. The arrow on the middle column indicated an example of cytochrome c release. Scale bar: 20 μm.
Of these hit compounds, N-(2-h
149x110mm (300 x 300 DPI)

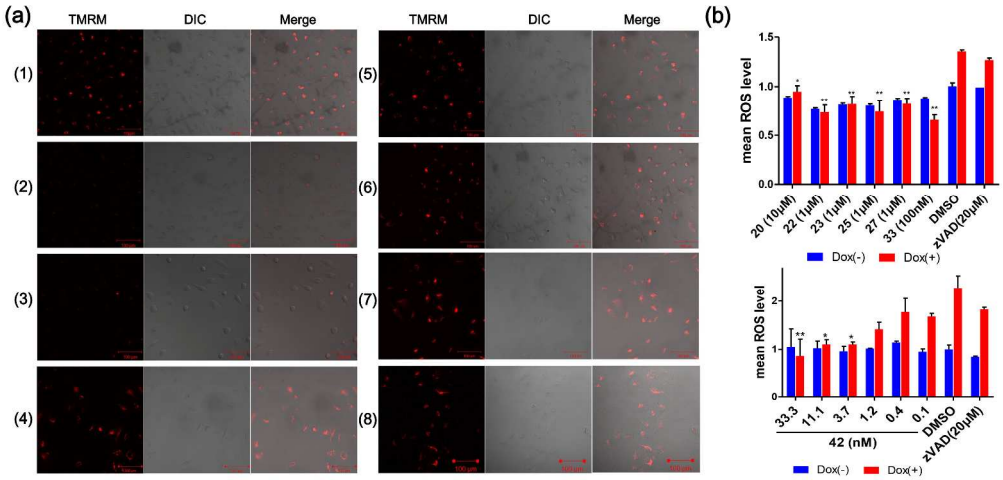

Figure 2. Mitochondrial protective effects of a series of apoptosis inhibitors. (a) TMRM staining of mitochondria in US2OS-Bim cells with (1),no apoptosis induction and treatment with DMSO, and with apoptosis inducted by the addition of DOX in the presence of the following treatments: (2), DMSO; (3), zVAD (10μM); (4), compound 20 (10μM); (5), compound 22 (1μM); (6), compound 23 (1μM); (7), compound 33 (100nM); (8), compound 42 (3 nM). Scale: 100 μm. (b) Mean cellular ROS levels in U2OS-Bim cells with (red bars) and without (blue bars) Dox induced apoptosis under the indicated compound treatments. Top: ROS levels under treatment with various apoptosis inhibitor compounds, DMSO, and zVAD. Bottom: ROS levels under treatment with different concentrations of compound 42, DMSO, and zVAD (20μM). The error bars represent the standard error of results from two separate experiments. P values are based on comparisons of each sample to the DMSO-treated apoptosis induction group. *: P<0.05; **: P<0.01; ***: P<0.001.

All of the tested compounds ma

388x184mm (300 x 300 DPI)

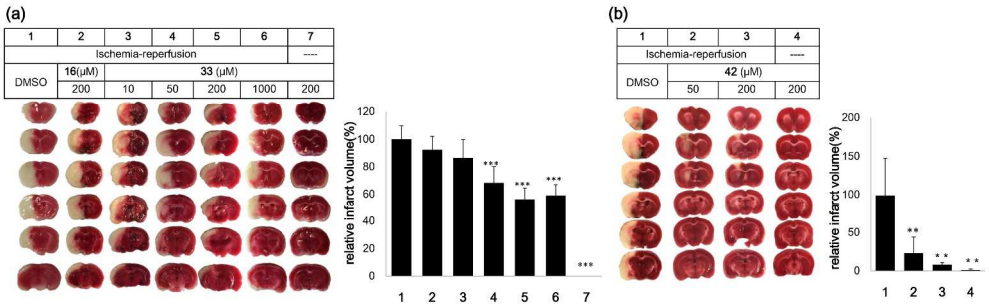

Figure 3. Compound 33(a) and compound 42 (b) have protective effects against ischemia-reperfusion injury. left: Representative 2, 3, 5-triphenyltetrazolium chloride (TTC) stained sections from middle cerebral artery occlusion (MCAO) brains injected with 5μl of the indicated concentrations of compounds 33 and 42. The white color represents the infarct and the red color represents the normal tissue. Right: Quantification of relative infarct volume. The numbers 1-7 on the x-axis correspond to the treatments in the top panel. Bars represent means ± standard deviation, n=3-6. P values are based on comparisons of each sample to the DMSO-treated ischemia-reperfusion(+) group.*: P,0.05; **: P<0.01; ***: P<0.001.
Evaluation of the brain infarc
392x118mm (300 x 300 DPI)